

## NUMERICAL STUDY AND REMEDIATION OF AC INTERFERENCE CORROSION ON NEIGHBOURING PIPELINES

F. BABAGHAYOU\*, B. ZEGNINI, T. SEGHER

Laboratory for the Study and Development of Semiconductors and Dielectric Materials,  
Amar Telidji University Laghouat, Algeria,

\*Corresponding Author: babag.fatiha@gmail.com

### Abstract

Buried pipelines for gas and oil are protected by an insulation coating and a Cathodic Protection (CP). However, neighbouring high voltage HV power lines induce an alternating current AC which causes corrosion damages on metallic structures, even in CP conditions, this phenomenon is known as the AC corrosion. In our study, we conducted a substantial theoretical research in this field to explain the basic electrical and electrochemical mechanisms of corrosion by AC. Afterwards; we performed numerical simulation studies of the electrochemical reactions involved in the corrosion, such as the anodic and cathodic processes, i.e., the iron oxidation and reduction of both oxygen and hydrogen. We also simulated the CP, AC corrosion, and deformation of the steel pipeline sample. Finally, in order to remedy this problem, we developed a monitoring and correction program for optimising the AC corrosion. In this article, we presented the study of the chemical behaviour of iron, oxygen and hydrogen. Moreover, we applied the rectification program, which did never exist in previous studies.

Keywords: AC corrosion, Cathodic protection, Electrochemical tests, Immunity zone, Reference potential.

## 1. Introduction

According to the ISO 8044-2000, corrosion is defined as a "physicochemical interaction between a metal and its environment resulting in changes in the properties of the metal and may lead to a significant deterioration in the function of the metal, the surrounding environment or their technical system" [1]. Buried pipelines are influenced by AC currents induced by high voltage overhead by both of an insulation coating and a Cathodic Protection (CP) and then serious damage by corrosion will take place.

More recently, some examples of corrosion caused by alternating current AC (50 Hz) on gas canalization were found [2]. The corrosion by AC of buried metallic structures has become a problem only in the last thirty years, following the growth in the number of so-called interference sources, for example, the traction systems and electrical transmission lines AC-powered, and of the structures buried pipes, for the transport of gases or oil, that share the path with the above-mentioned sources for long distances because of the space limitation imposed by private or governmental entities [3, 4]. In recent decades, the improvement of the insulation capacity of the cathodically-protected pipe coatings has aggravated the problem of corrosion by AC: the passage to the use of the bitumen and particularly polyethylene and polypropylene extruded, allowed to increase the electrical resistivity of the coatings and to minimise the size and the number of defects. This is an advantage because it reduces the current CP to be delivered but causes at the defects area high densities of interfering AC. This is considered by many authors as one of the main reasons for the growth in the number of cases of corrosion attributable to the interference by AC [4-9] And a substantial studies have been carried out in this field, by many researchers as Brenna et al [3], Nielsen et al. [6], Christoforidis et al. [9], Gupta et al [10], Ding and Fan [11], Ibrahim et al [12], Yan et al [13] and NACE International [14].

In gas and oil companies, a serious AC corrosion problem of buried pipelines has been confronted, even in a protection condition by both of an insulation coating and a Cathodic Protection (CP). To remedy the problem, the companies are opting to replace defective sections, which is economically very costly.

To resolve this problem, our research goals are to simulate this phenomenon and conducting investigations which are summed up in three points; first, we conducted a theoretical research to explain the basic electrical and electrochemical mechanisms of corrosion by the alternating current, the second point is carrying out an electrochemical tests on a laboratory model by using a sample of pipeline steel type API 5L X52, which is used in Algeria; for realizing our experimental investigation, we used an advanced electrochemical workstation potentiostat and galvanostat EC-LAB VSP300. It allowed us to simplify the model of the studied phenomenon, and it provided all of our measurements, we used a test cell containing a pipeline's sample, and a solution to simulate the electrolyte.

The test cell was first subjected to measurements of the free potential, which means without the both of CP and AC and secondly, we applied to the sample a DC as CP, the measurements of the reference potential  $E_{off}$  close to the iron sample allowed us to select an appropriate CP, then we added an AC current in order to simulate the induced current. The results have shown that the induced AC current causes the corrosion of the sample even in Cathodic Protection condition [15, 16]. The third point, we did simultaneously with the second one, is a numerical simulation

study in order to digitally represent the test cell, the CP phenomenon and the AC corrosion, we also suggested an efficient solution for minimising its impact on pipelines. This numerical simulation of the process was possible by using the COMSOL Multiphysics software [17-20], we introduced all parameters of both of the iron sample and the electrolyte simulating. We measured the  $E_{off}$ , we selected the appropriate CP, which brings the immunity state, and then we added AC for simulating induced current. In this last case, the measured results gave an  $E_{off}$  exceeding the immunity zone regarding standards [8, 21, 22], a strong oxidation of iron, a significant reduction of oxygen, a high liberation of hydrogen and a clear sample deformation.

All these results mean that our sample of the pipeline, which was protected by CP, when it was subjected to an induced AC its corrosion, took place. These numerical results validate the experimental study results. Finally, we have set up a monitoring and correction program to bring the  $E_{off}$ , in the presence of AC, in the immunity corrosion zone according to standards; our monitoring program was able to minimize the reactions of the electrochemical process and it prevented the sample's deformation, because it can testing, calculating and choosing automatically in each case a safety CP. This article is dedicated to the explanation of the study of the numerical simulation part.

## 2. Theoretical Study of Corrosion by AC

We conducted a conscientious theoretical research, it showed us the main AC corrosion mechanism of pipelines API type, it illustrated to us multiple points such as the different types of AC interference [3], the corrosion by AC [3, 22], the explanation of electrochemical corrosion, [23], the standards, the pourbaix diagram (as shown in Fig. 1) of corrosion and immunity areas [3, 4, 21], the Cathodic Protection [3, 23], the measurement parameters of corrosion [3] and the principal models of the corrosion mechanism by AC [24].

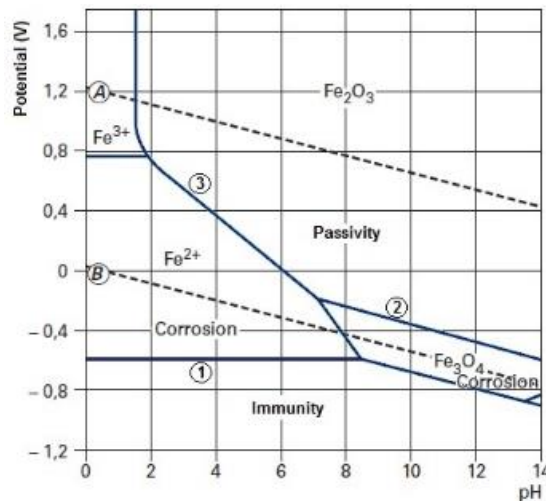
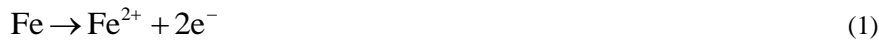


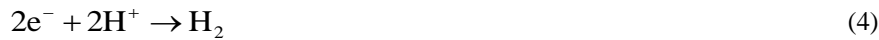
Fig. 1. Iron pourbaix diagram of corrosion and immunity areas [3, 21].

Below the reactions of the electrochemical process [2, 3, 23, 24]:

Anodic process:



Cathodic process:



The topics studied in the theoretical part are:

- AC interferences.
- Electrochemical corrosion of steel.
- Pourbaix diagrams.
- Cathodic protection.
- Thermodynamic effect.
- Kinetic effect.
- Chemical effect.
- Cathodic Protection monitoring.
- AC corrosion, characteristics.
- AC Cathodic Protection criteria.
- AC corrosion monitoring.
- AC interference mitigation.
- Models of the AC corrosion mechanism, such as model extracted from technical specification CEN / TS 15280, equivalent electrical circuit model, electrochemical model, mathematical models and AC tidal effect model.

### 3. Numerical Modelling

We did a simulation study in order to, digitally represent the CP phenomenon, AC corrosion and optimizing AC corrosion behaviour by changing the CP in case of AC interferences, by a monitoring program, which returns process status to the immunity zone, by referring to pourbaix diagram and CP criteria suggested by Hosokawa [3, 8, 21, 22]. The immunity zone is  $-1.15 \text{ V} < E_{off} < -0.85 \text{ V}$ , where  $E_{off}$  is the reference potential sensed by the reference electrode. Numerical simulations are based on:

#### 3.1. The model geometry

The model geometry used in the simulation part contains the sample, the electrode and the electrolyte as shown in Fig. 2.

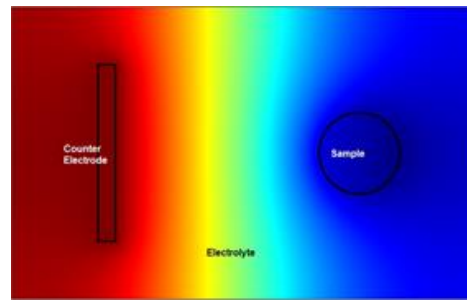


**Fig. 2. The model geometry (sample, counter electrode and electrolyte).**

This simulation requires:

The configuration of parameters initial value [17-20]: Electrolyte conductivity; Diffusion coefficient of *Fe* (iron), *O<sub>2</sub>* (oxygen) and *H<sub>2</sub>* (hydrogen), Tafel slope iron oxidation, hydrogen evolution and oxygen reduction, Reference concentration of *Fe*, *O<sub>2</sub>* and *H<sub>2</sub>*, iron oxidation equilibrium potential, hydrogen evolution equilibrium potential, oxygen reduction equilibrium potential, iron oxidation exchange current density, hydrogen evolution current density and oxygen reduction exchange current density.

The definition and the electrochemical composition of iron API 5L X52 pipeline used in Algeria (sample in Fig. 2) in the "Material Overview" COMSOL section [17-20]: Thermal conductivity (W/(m.K)), Resistivity (Ω.m), Surface emissivity, Coefficient of thermal expansion (1/K), Heat capacity at constant pressure (J/(kg.K)), HC (J/(mol.K)), Electrical conductivity (S/m), Density (kg/m<sup>3</sup>), VP (Pa), Tangent coefficient of thermal expansion (1/K), Thermal strain, Isotropic tangent coefficient of thermal expansion (1/K), Isotropic thermal strain, Young's modulus (Pa), Poisson's ration, Bulk modulus (N/m<sup>3</sup>) and Shear modulus (N/m<sup>3</sup>).

The definition of the reference electrode is in the "Domain Probe– Definition" COMSOL section [17-20]: The Probe, Probe type, Source application (Sample surface), Calculation type (average).

The definition of the electrolyte used (*NaCl + Na<sub>2</sub>SO<sub>4</sub>*) is in the "Material" COMSOL section [17-20]: Thermal conductivity (W/(m.K), Heat capacity at constant pressure (J/(kg.K), HC (J/(mol.K) and VP (Pa).

### 3.2. The parameterization of current distribution in the cell

The electrode is a metallic conductor, thus its current-voltage relation is obeyed to ohm's law [21, 25, 26]:

$$i_s = -\sigma_s \nabla \Phi_s \quad \text{with} \quad \nabla \cdot i_s = Q_s \quad (5)$$

where *i<sub>s</sub>* is the current density (A/m<sup>2</sup>) in the electrode, *σ<sub>s</sub>* is the conductivity (S/m), *Φ<sub>s</sub>* is the electric potential (V), and *Q<sub>s</sub>* is the general current source term (A/m<sup>3</sup>).

The electric potential *Φ<sub>s</sub>* is defined as [3, 27]:

$$\Phi_s = E_{CP} + E_{AC} = E_{CP} + A.\sin(2\pi.f.t) \quad (6)$$

where  $E_{CP}$  is the applied potential of CP,  $E_{AC}$  is the AC potential,  $A$  is the amplitude of the AC potential and  $f$  is the frequency (50 Hz).

The electrolyte, which is an ionic conductor, the net current density can be described, using the sum of fluxes of all ions [21, 26]:

$$i_l = F \sum_i z_i . N_i \quad (7)$$

where  $i_l$  is the current density (A/m<sup>2</sup>) in the electrolyte,  $F$  is Faraday constant (C/mol), and  $N_i$  is the flux of species  $i$  (mol.(m<sup>2</sup>/s)) with charge number  $z_i$ .

The flux of an ion in an ideal electrolyte solution is described by the nernst-planck equation and accounts for the flux of solute species by diffusion, migration, and convection in the three respective additive terms [21, 26]:

$$N_i = -D_i \nabla c_i - z_i u_{m,i} F c_i \nabla \Phi_l + c_i u \quad (8)$$

where for the specie  $i$ ,  $c_i$  is the concentration (mol/m<sup>3</sup>),  $D_i$  is the diffusion coefficient (m<sup>2</sup>/s),  $u_{m,i}$  is its mobility (s.mol/kg),  $\Phi_l$  is the electrolyte potential (V), and  $u$  is the velocity vector (m/s).

On substituting the nernst-planck equation into the expression for current density, we find [21, 26]:

$$i_l = -F \left( \nabla \sum_i z_i D_i c_i \right) - F^2 \nabla \Phi_l \sum_i z_i^2 u_{m,i} c_i + u F \sum_i z_i c_i \quad (9)$$

$$\text{with conservation of current: } \nabla . i_l = Q_l$$

This general treatment of electrochemical theory is usually too complicated to be practical. By assuming that one or more of the terms in Eq. (9) are small, the equations can be simplified and linearized [21, 25, 26, 28, 29]:

$$i_l = -\sigma_l \nabla \Phi_l \text{ with } \nabla . i_l = Q_l \quad (10)$$

The difference between the actual potential difference and the equilibrium potential difference is the activation overpotential  $\eta$  (electrode-electrolyte-interface) [21, 26, 28, 29, 30]:

$$\eta = Q_s - Q_l - E_{eq} \quad (11)$$

where  $E_{eq}$  is the equilibrium potential and it is given by nernst's equation [3]:

$$E_{eq} = E_0 + K . \log \left( \frac{a_{M^{z+}}}{a_M} \right) \quad (12)$$

### 3.3. The transport of chemical species

In order to configure the concentration and the chemical species movement (Fe, O<sub>2</sub>, H<sub>2</sub>) [31], the driving forces for transport can be diffused by Fick's law, convection when coupled to a flow field, and migration, when coupled to an electric field [26].

$$(\sigma_i / \sigma) + \nabla(-D_i \nabla c_i) + u \cdot \nabla c_i = R_i \tag{13}$$

where for the specie  $i$ ,  $c_i$  is the concentration (mol/m<sup>3</sup>),  $D_i$  is the diffusion coefficient (m<sup>2</sup>/s),  $u$  is the velocity vector (m/s), and  $R_i$  is the reaction rate expression (mol/(m<sup>3</sup>.s)).

The flux vector  $N$  is associated with the mass balance equation above and used in boundary conditions and flux computations. For the case where the diffusion and convection are the only transport mechanisms, the flux vector is defined as [26]:

$$N_i = -D_i \nabla c_i + u c_i \tag{14}$$

### 3.4. The math ODE and DAO

We used this module in COMSOL multi-physics to support the monitoring program Fig. 3 in order to bring the situation to the immunity state, below the simplified algorithm used:

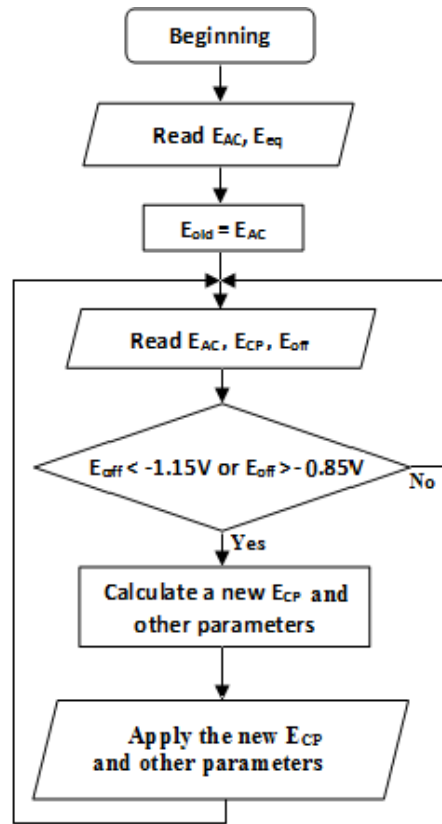


Fig. 3. Simplified program to return in the immunity zone.

The basic idea of the immunity program resides in its function as a monitor controller, it loops indefinitely so that the system (the sample, CP and  $E_{off}$ ) stays continually under monitoring.

As long as there is no overrun of  $E_{off}$  of the immunity zone limits ( $-1.15V < E_{off} < -0.85 V$ ) the program loops without doing anything. But, in case of overcoming, the program rectifies the CP, taking into consideration the previous value of CP and the sensed values of  $E_{off}$  and AC, until the  $E_{off}$  returns to the immunity area.

### 3.5. The deformation of the sample by corrosion

We applied the corrosion-secondary model wizard of COMSOL to our model [17-20]. It is a predefined multiphysics interface that contains an interface for the electric current distribution and an interface for deformed geometry. The last handle the deformed geometry part of the problem.

For the counter electrode surface, which was not deformed, we used an electrode surface node to model the reduction reaction. For the sample surface, we used an electrode surface node with an added dissolving-depositing species, which set up both the deformation of the geometry and the steel electrode reactions.

We also solved the model using a time-dependent study with automatic remeshing enabled [17-20].

Based on the cathodic tafel expression to describe the kinetics of the reaction and anodic Tafel expression for the anodic electrode reaction current density [28, 30, 32-35]:

$$i_{cat} = -i_{0,cat} \cdot 10^{\frac{\eta}{A_{cat}}}, \quad i_{tafel} = -i_{0,an} \cdot 10^{\frac{\eta}{A_{an}}} \quad (15)$$

$$i_{an} = \frac{(i_{tafel} \cdot i_{lim})}{(i_{tafel} + i_{lim})} \quad (16)$$

where  $i_0$  is the exchange current density,  $\eta$  is the overpotential of the reaction and  $A_{an}$   $A_{cat}$  are the Tafel slope, and  $i_{lim}$  is limiting current density.

The dissolution of iron metal makes the electrode boundary moving, with a velocity in the normal direction,  $v$  (m/s), according to:

$$v = \left( \frac{i_{an}}{2F} \right) \left( \frac{M}{\rho} \right) \quad (17)$$

where  $M$  is the average molar mass,  $\rho$  is the density of the iron,  $F$  is the Faraday const. (C/mol).

## 4. Results and Discussion

### 4.1. The potential $E_{off}$ in the presence of CP

Figures 4 to 9 represent the  $E_{off}$  in the presence of CP and for different values of an induced current AC, without than with the immunity program, this representation allowed us to discuss, following the curves of the corrosion of the sample, based on the standards [1, 3, 8, 21, 22].



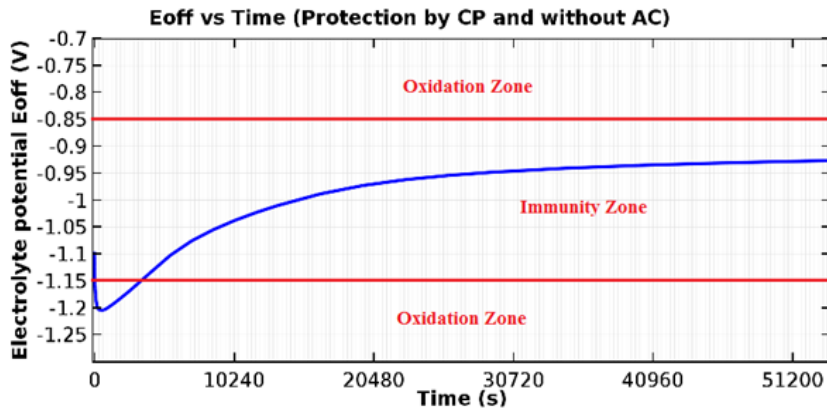


Fig. 4.  $E_{off}$  in the presence of CP and without AC.

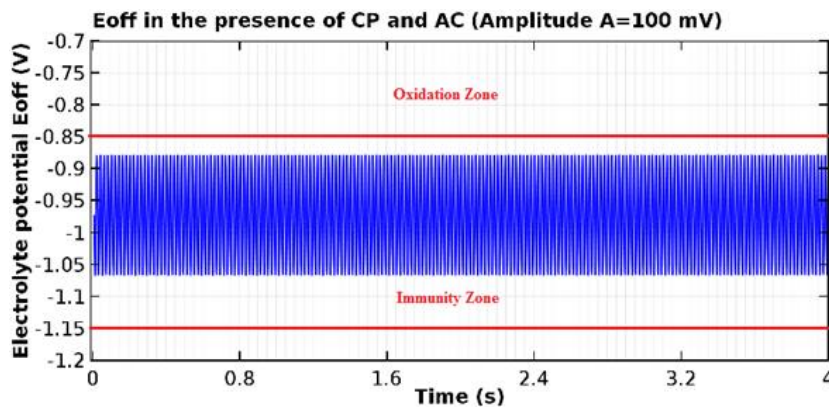


Fig. 5.  $E_{off}$  in the presence of CP and AC (amplitude  $A=100$  mV).

Figure 4 represents the measured  $E_{off}$  in the presence of a right CP without the presence of induced current AC, we brought the  $E_{off}$  in the immunity area by choosing the adequate CP, regarding the standards [1, 3, 8, 21, 23]. Figure 5 shows that the potential  $E_{off}$  in the presence of CP and AC (amplitude  $A=100$  mV) did not exceed the immunity zone, in this case, we did not need to modify the CP.

Figure 6 (amplitude  $A=200$  mV) illustrates that  $E_{off}$  exceeded the immunity area, therefore there is a significant risk of corrosion. Then in Fig. 7, for the same values of AC and by introducing the resolution of the immunity program Fig. 3, we were able to bring the  $E_{off}$  in immunity zone. Secondly, we measured the concentration of the different species of the electrochemical process.

Figure 8 (amplitude  $A=500$  mV) illustrates that  $E_{off}$  exceeded the immunity area, therefore there is a significant risk of corrosion. Then, in Fig. 9, for the same values of AC and by introducing the resolution of the immunity program Fig. 3, we were able to bring the  $E_{off}$  in immunity zone. Secondly, we measured the concentration of the different species of the electrochemical process.

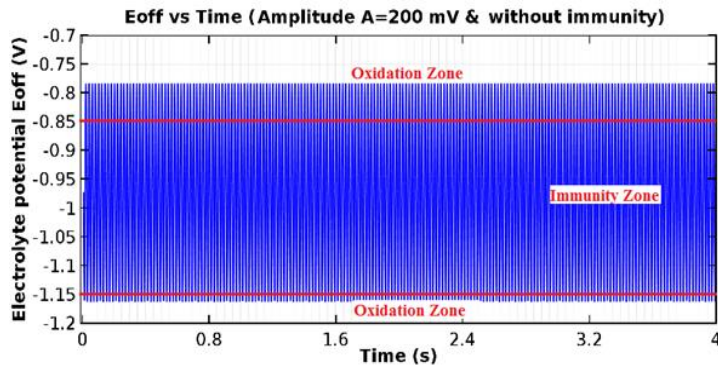


Fig. 6.  $E_{off}$  in the presence of CP and AC (amplitude  $A=200$  mV) without application of immunity program.

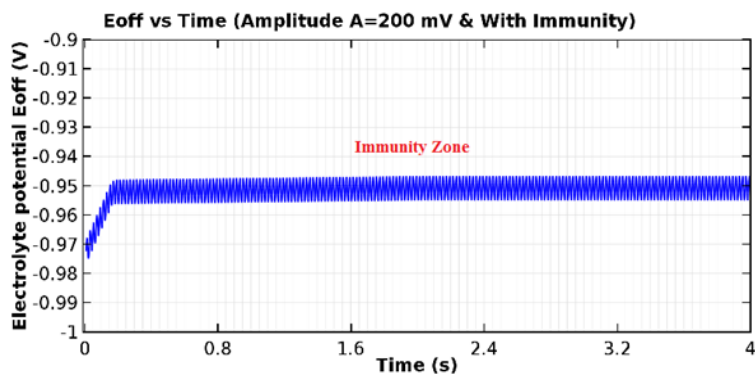


Fig. 7.  $E_{off}$  in the presence of CP and AC (amplitude  $A=200$  mV) with application of immunity program.

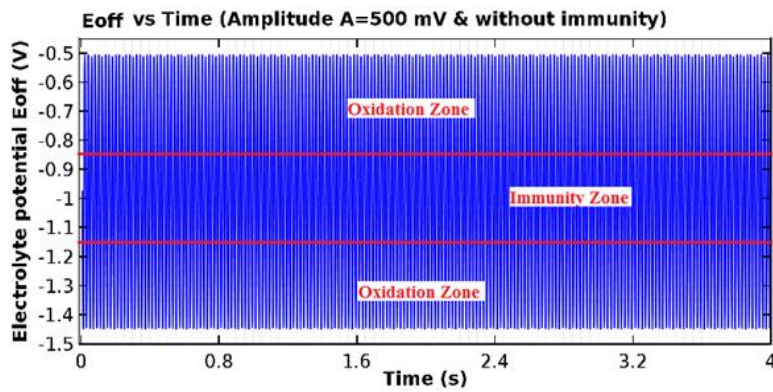


Fig. 8.  $E_{off}$  in the presence of CP and AC (amplitude  $A=500$  mV) without application of immunity program.

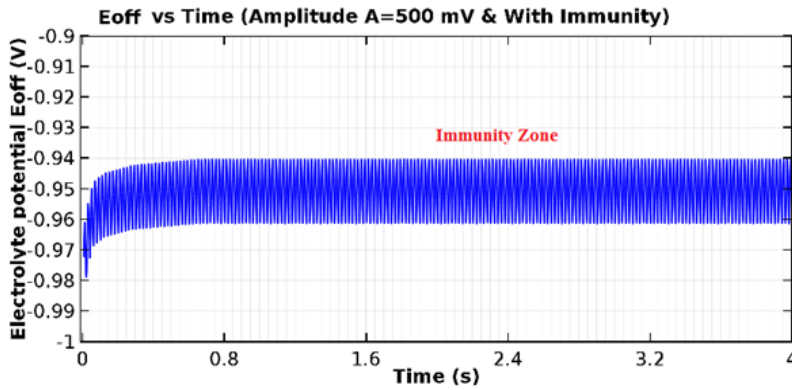
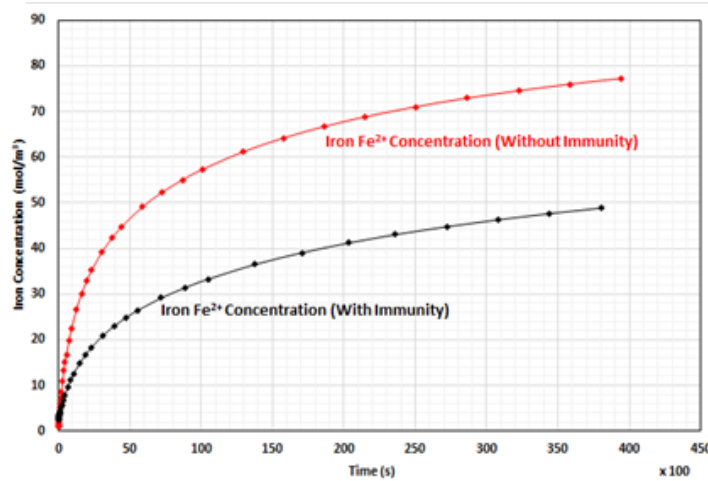


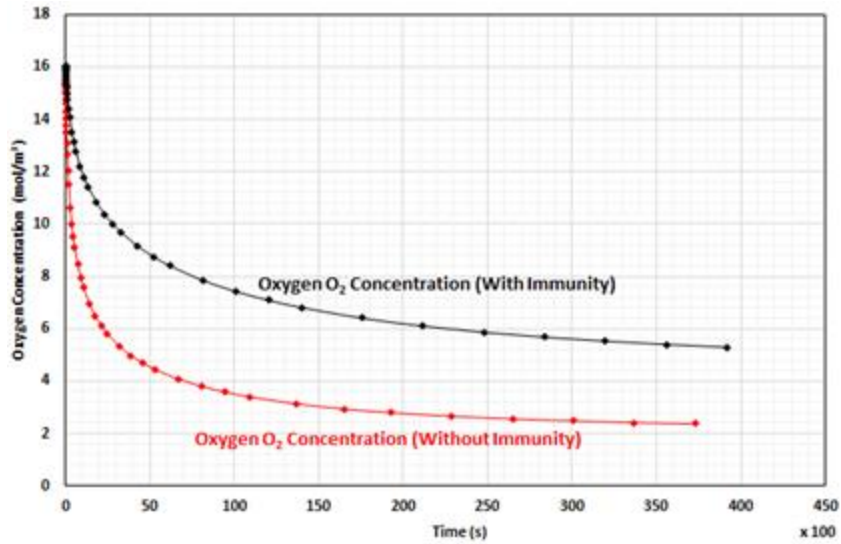
Fig. 9.  $E_{off}$  in the presence of CP and AC (amplitude  $A=500$  mV) with application of immunity program.

**4.2. The concentration of iron ions, oxygen and hydrogen**

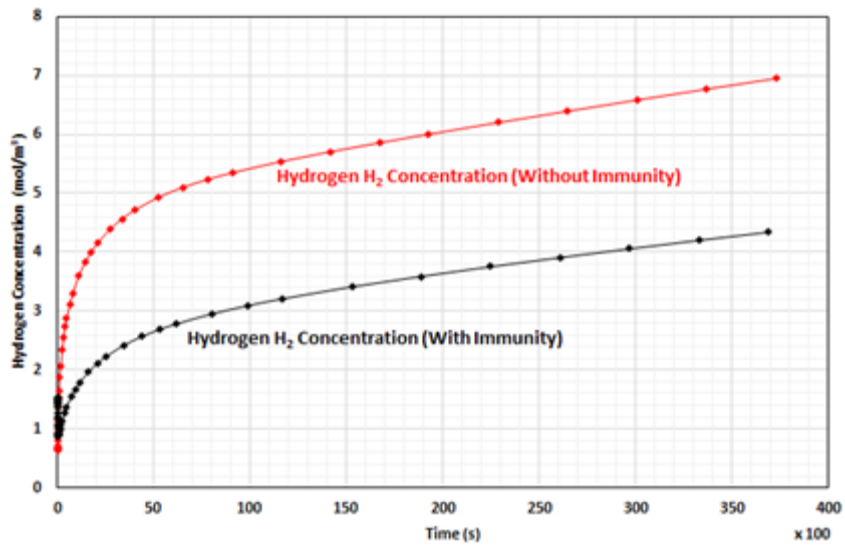
Figure 10(a) shows the increase of the iron ions  $Fe^{2+}$  concentration near the sample, thus demonstrating that a reaction of oxidation of iron Eq. (1), so the corrosion took place. And after the implementation of the immunity program Fig. 3, this concentration decrease. Figure 10(b) illustrates the important decrease of the oxygen  $O_2$  concentration near the sample, thus demonstrating a reaction of oxygen reduction Eq. (2), so it is a case of a strong corrosion. In addition, after the implementation of the immunity program Fig. 3, this concentration increase. And Fig. 10(c) shows the increase of the hydrogen  $H_2$  concentration near the sample, it demonstrates that it is a reaction of reduction of  $H_2O$  Eq. (3) or  $H^+$  Eq. (4), so an important corrosion, took place. And after the implementation of the immunity program Fig. 3, this concentration decrease.



(a) Concentration of iron ions  $Fe^{2+}$ .



(b) Concentration of O<sub>2</sub>.



(c) Concentration near sample of H<sub>2</sub>.

Fig. 10. Concentration near sample of Fe<sup>2+</sup>, O<sub>2</sub> and H<sub>2</sub>.

### 4.3. The sample deformation under CP and AC

Finally, we studied the sample deformation protected by CP and under AC, Fig. 11 shows the restriction of the model just to view clearly the sample deformation, Fig. 12 shows a clear deformation by corrosion of the sample which was protected by CP and subjected to an induced AC, and in Fig. 13 when we apply our immunity program during the same time period (72 hours) we did not have any deformation yet.

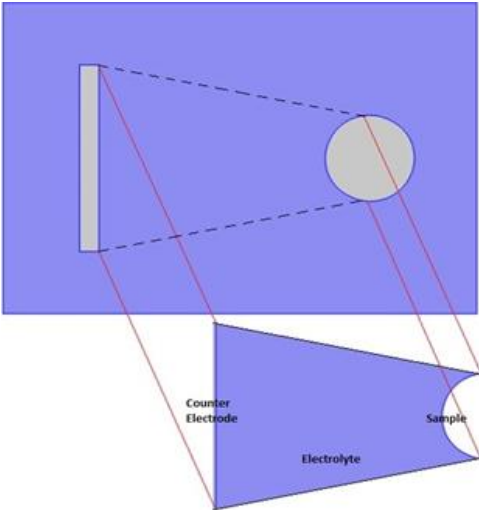


Fig. 11. Model restriction.

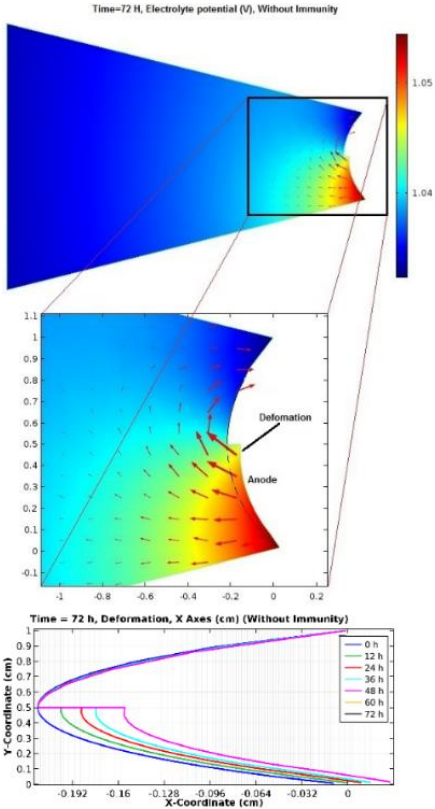
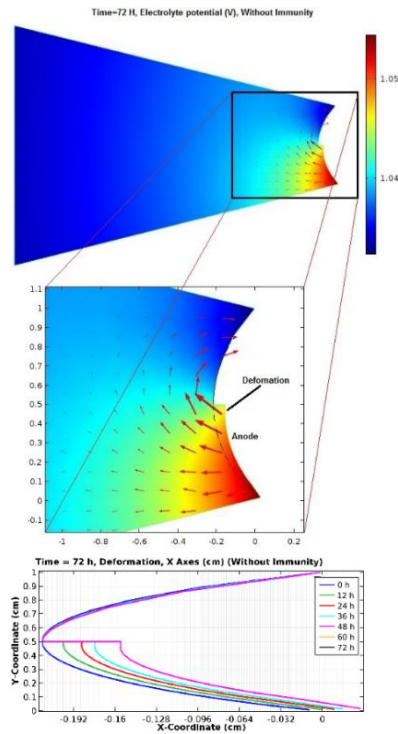


Fig. 12. Sample deformation by corrosion (under CP and AC).



**Fig. 13. Deformation state after implementation of the return program to the immunity zone.**

## 5. Conclusions

In conclusion, regarding the numerical simulation, the results indicated that the induced AC current causes the corrosion of the sample, which was protected by the CP because we found an  $E_{off}$  exceeding the immunity zone and a strong oxidation of iron. We have also simulated the oxygen and the hydrogen concentration in the electrolyte, and the sample deformation. Then, using our monitoring program has allowed us to bring the  $E_{off}$ , in the presence of AC in corrosion immunity zone according to standards, to decrease the reactions of the electrochemical process and it equally prevents the sample's deformation.

The direct links between the experimental and simulation study are that we have used the same steel (API 5L X52); The potential applied to the studied sample obeyed to the same formula, it was equal to the addition of a direct current as a CP and an alternating current as AC interference; Results have shown that the experimental data are relatively in agreement with simulation ones; The execution of the monitoring and corrective program of CP in case that the  $E_{off}$  exceeds the limits is possible in the simulation but experimentally it is not possible by the used device, the potentiostat and galvanostat.

To sum up, in our future perspective, our goal is to establish a system provided with a microcontroller to monitor the CP and for implementing the immunity program in addition to the existing CP system in places where pipelines are near power lines and causing interference AC.

## Acknowledgements

We would like to thank laboratory of process engineering department and laboratory of mechanics, Amar Telidji University of Laghouat, Algeria and ENS (Higher normal school of Laghouat) for EC-LAB. The authors thank Professor Mr. Madjid TEGUARA, Research laboratory of electrical engineering, National Polytechnic, B.P 182, El-Harrach, Algeria for COMSOL code.

### Nomenclatures

$A$	Amplitude of the AC potential, mV
$A_{an}$	Tafel slope anodic
$A_{cat}$	Tafel slope cathodic
$a_M$	Metal activity in the electrolyte
$a_M^{Z+}$	Metallic ions activity
$c_i$	Concentration, mol/m <sup>3</sup>
$D_i$	Diffusion coefficient, m <sup>2</sup> /s
$E_0$	Metal standard potential, mV
$E_{AC}$	AC potential, mV
$E_{CP}$	Applied potential of CP, mV
$E_{eq}$	Equilibrium potential, mV
$E_{off}$	Reference potential, mV
$F$	Faraday constant, C/mol
$f$	Frequency, Hz
$i_0$	Exchange current density, A/m <sup>2</sup>
$i_l$	Current density in the electrolyte, A/m <sup>2</sup>
$i_{lim}$	Limiting current density, A/m <sup>2</sup>
$i_s$	Current density in the electrode, A/m <sup>2</sup>
$K$	Constant
$M$	Average molar mass
$N$	Flux vector, mol/(m <sup>2</sup> .s)
$N_i$	Flux of species $i$ , mol.(m <sup>2</sup> /s)
$Q_s$	General current source term, A/m <sup>3</sup>
$R_i$	Reaction rate expression, mol/(m <sup>3</sup> .s)
$u$	Velocity vector, m/s
$u_{m,i}$	Mobility, s.mol/kg
$z_i$	Charge number

### Greek Symbols

$\sigma_s$	Conductivity, S/m
$\rho$	Density of the iron
$\Phi_s$	Electric surface potential, V
$\Phi_l$	Electrolyte potential, V
$\eta$	Over-potential of the reaction V

### Abbreviations

AC	Alternating Current
CP	Cathodic Protection
DC	Direct Current
HV	High Voltage

## References

1. Barbalat, M. (2012). *Apport des techniques électrochimiques pour l'amélioration de l'estimation de l'efficacité de la protection cathodique des canalisations enterrées*. Ph.D. Thesis. Materials Engineering, Université de La Rochelle, France.
2. Biase, L.D. (2001). *Guideline for the corrosion protection of pipelines, Guideline for the corrosion protection of pipelines*. CeoCor.
3. Brenna, A.; Lazzari, L.; and Castiglioni, C. (2012). *A proposal of AC corrosion mechanism of carbon steel in cathodic protection condition*. Ph.D. Thesis. Department of Chemistry, Materials and Chemical Engineering, Polytechnic of Milan, Milan, Italy.
4. Hosokawa, Y.; Kajiyama, F.; and Nakamura, Y. (2004). New cathodic protection criteria based on direct and alternating current densities measured using coupons and their application to modern steel pipeline. *Corrosion*, 60(3), 304-312.
5. Daniel, W.C.; and Richard, W.B. (2016). *Ductile iron pipe research association, Dipra*.
6. Nielsen, L.V.; Nielsen, K.V.; Baumgarten, B.; Breuning-Madsen, H.; Cohn, P.; and Rosenberg, H. (2004). AC induced corrosion in pipelines: detection, characterization and mitigation. *Proceedings of the NACE International Conference on Corrosion*. New Orleans, Louisiana, 04211.
7. Kioupi, N.; and Maroulis, K. (2006). AC-corrosion detection on electrical resistance probes connected to a natural gas transmission pipeline. *Proceedings of the 8th International Conference Pipeline Rehabilitation and Maintenance*. Istanbul, Turkey.
8. Hosokawa, Y.; Kajiyama, F.; and Nakamura, Y. (2006). Overcoming the new threat to pipeline integrity-AC corrosion assessment and its mitigation. *Proceedings of the 23rd World Gas Conference*. Amsterdam, Netherlands, 641.
9. Christoforidis, G.C.; Labridis, D.P.; and Dokopoulos, P.S. (2003). Inductive interference calculation on imperfect coated pipelines due to nearby faulted parallel transmission lines. *Electric Power Systems Research*, 66, 139-148.
10. Gupta, R.K.; Tan, M.Y.J.; Esquivel, J.; and Forsyth, M. (2016). Occurrence of anodic current and corrosion of steel in aqueous media under fluctuating cathodic protection potentials. *Corrosion*, 72(10), 1243-1251.
11. Ding, Q.; and Fan, Y. (2016). Experimental study on the influence of AC stray current on the cathodic protection of buried pipe. *International Journal of Corrosion*, Article ID 561392, 8 pages.
12. Ibrahim, I.; Tribollet, B.; Takenouti, H.; and Meyer, M. (2015). AC-induced corrosion of underground steel pipelines. faradaic rectification under cathodic protection: i. theoretical approach with negligible electrolyte resistance. *Journal of the Brazilian Chemical Society*, 26(1), 196-208.
13. Yang, Y.; Wang, S.; and Wen, C. (2016). Experimental study on alternating current corrosion of pipeline steel in alkaline environment. *International Journal of Electrochemical Science*, 11(8), 7150-7162.
14. NACE SP0177. (2007). Mitigation of alternating current and lightning effects on metallic structures control system. *NACE International Standard Practice*.



15. Babaghayou, F.; Zegnini, B.; and Seghier, T. (2016). Experimental model investigation of the corrosion of buried steel pipelines with cathodic protection near high voltage power lines. *Proceedings of the IEEE International Conference on Electrical Sciences and Technologies in Maghreb (CISTEM)*. Morocco, Marrakech, 1-6.
16. Babaghayou, F.; Zegnini, B.; and Seghier, T. (2016). Study of corrosion by alternating currents on buried and cathodically protected pipelines near high-voltage power lines. *Materials Research Proceedings*, 1, 122-126.
17. COMSOL A.B. (2010) COMSOL multiphysics user' guide version 4.1. California: COMSOL Inc.
18. Gongadze, E.; Petersen, S.; Beck, U.; and Van-Rienen, U. (2009). Classical models of the interface between an electrode and an electrolyte. *Proceedings of the COMSOL Conference*. Netherlands, Grenoble, 14-16.
19. Peelen, W.H.A.; and Courage, W.M.G. (2007). An advanced finite element reliability tool for stray current corrosion assessments. *Proceedings of the COMSOL Users Conference*. Grenoble.
20. Mizuno, D.; Shi, Y.; and Kelly, R. (2011). Modelling of galvanic interactions between AA5083 and steel under atmospheric condition. *Proceedings of the COMSOL Worldwide Conference*. Boston.
21. Nichols, P.; Holtsbaum, B.; Mayfield, D.; Nelson, S.; Parker, K.; Schramm, D.A.; and Zurbuchen, S. (2008). CP3-cathodic protection technologist course manual. *NACE International Training and Certification*.
22. Nguyen-Thuy, L.E. (2008). *Protection cathodique*. INERIS. 41 pages.
23. Wakelin, R.G.; Gummow, R.A.; and Segall, S.M. (1998). AC corrosion - case histories test procedures and mitigation. *Proceedings of the Corrosion NACE International Conference*. San Diego, United States of America, Paper 98565.
24. Hosokawa, Y.; Kajiyama, F.; and Nakamura, Y. (2002). New CP criteria for elimination of the risks of AC corrosion and overprotection on cathodically protected pipelines. *Proceedings of the Corrosion NACE International Conference*. Denver, United States of America, Paper 02111.
25. Ludwig, R.; Leuenberger, G.; Makarov, S.; and Apelian, D. (2002). Electric voltage predictions and correlation with density measurements in green-state powder metallurgy compacts. *Journal Nondestructive Evaluation*, 21(1), 1-8.
26. Kofstad, P.; and Norby, T. (2007). *Defects and transport in crystalline solids*. Compendium for the advanced level course. Department of Chemistry, University of Oslo.
27. BioLogic; EC-Lab. (2011). *Software, techniques and applications*. BioLogic Science Instruments.
28. Deshpande, K.B. (2010). Validated numerical modelling of galvanic corrosion for couples: magnesium alloy (AE44)-mild steel and AE44-aluminium alloy (AA6063) in brine solution. *Corrosion Science*, 52(10), 3514-3522.
29. Freda, M.; Giannetti, A.; Lattanzi, L.; and Luperi, S. (2013). Electrochemical pickling of steel for industrial applications: Modelling. *Proceedings of the COMSOL Conference*. Rotterdam.

30. Muehlenkamp, E.B.; Koretsky, M.D.; and Westall, J.C. (2012). Effect of moisture on the spatial uniformity of cathodic protection of steel in reinforced concrete. *Corrosion*, 61(6), 519-533.
31. Muehlenkamp, E.B. (2005). *Electrochemical modelling of cathodic protection systems applied to reinforced concrete structures*. Master Thesis. Chemical Engineering, Oregon State University, United States of America.
32. Hinds, G. (2008). *The electrochemistry of corrosion*. Edited by Gareth Hinds from the original work of J.G.N. Thomas. National Physical Laboratory Teddington. 15 pages.
33. Abdulsalam, M.I.; and Pickering, H.W. (1998). The effect of crevice-opening dimension on the stability of crevice corrosion for nickel in sulfuric acid. *Journal of the Electrochemical Society*, 145(7), 2276-2284.
34. Brackman, M.; Clemons, C.B.; Golovaty, D.; and Kreider, K.L. (2012). Modelling and computational simulation of crevice corrosion damage evolution. *Proceedings of the NACE Corrosion Conference*, Utah, United States of America.
35. Deshpande, K.B. (2012). Effect of aluminium spacer on galvanic corrosion between magnesium and mild steel using numerical model and SVET experiments. *Corrosion Science*, 62(9), 184-191.